IL NUOVO CIMENTO Vol. 37 C, N. 1 Gennaio-Febbraio 2014
DOI 10.1393/ncc/i2014-11693-6

Colloquia: IFAE 2013

Measurements of the properties of the Higgs-like boson in the four leptons decay channel with the ATLAS detector using 25 fb^{-1} of proton-proton collision data

E. Rossi(*) on behalf of the ATLAS Collaboration
Sapienza Università di Roma - Roma, Italy

ricevuto l'1 Ottobre 2013

Summary. — An update of the search results and the measurement of the properties of the newly observed Higgs-like particle in the decay channel $H \to ZZ^{(*)} \to \ell^+\ell^-\ell'^+\ell'^-$, where ℓ, $\ell' = e$ or μ, using proton-proton (pp) collision data recorded with the ATLAS detector at the Large Hadron Collider (LHC) is presented. This analysis uses the full 2011 and 2012 pp collision datasets of 4.6 fb^{-1} and 20.7 fb^{-1} at $\sqrt{s} = 7$ TeV and 8 TeV, respectively. A clear excess of events over the background is observed at $m_H = 124.3$ GeV with a significance of 6.6 standard deviations, corresponding to a background fluctuation probability of 2.7×10^{-11}. This paper is focused on the first measurements of the signal strength, mass, spin-parity and couplings.

PACS 14.80.Bn – Standard-model Higgs bosons.

1. – Introduction

The search for the Standard Model (SM) Higgs boson [1] is one of the most important aspects of the Large Hadron Collider (LHC) physics programme. The study of the decay channel $H \to ZZ^{(*)} \to \ell^+\ell^-\ell'^+\ell'^-$, where ℓ, $\ell'' = e$ or μ, provides good sensitivity over a wide mass range. The main background to this search comes from continuum $(Z^{(*)}/\gamma^*)(Z^{(*)}/\gamma^*)$ production, referred to as $ZZ^{(*)}$ hereafter. For $m_H < 180$ GeV, there are also non-negligible background contributions from $Z +$ jets and $t\bar{t}$ production.

This paper is focused on the first measurements (signal strength, mass, spin-parity and couplings) of the newly observed Higgs-like particle in the $H \to ZZ^{(*)} \to 4\ell$ channel based on 4.6 fb^{-1} at $\sqrt{s} = 7$ TeV and 20.7 fb^{-1} at $\sqrt{s} = 7$ TeV pp collision data recorded by the ATLAS detector [2].

(*) E-mail: elvira.rossi@cern.ch; elly@na.infn.it

2. – The ATLAS Detector

The ATLAS experiment uses a general purpose detector consisting of an inner tracker, a calorimeter and a muon spectrometer. The inner detector (ID) directly surrounds the interaction point; it includes a silicon pixel detector, a silicon strip detector and a transition radiation tracker, and is embedded in a 2 T magnetic field. The ID ($|\eta| < 2.5$) is enclosed by a calorimeter system containing electromagnetic and hadronic sections. The calorimeter is surrounded by a large muon spectrometer inside an air-core toroid magnet system which contains a combination of monitored drift tubes and cathode strip chambers, designed to provide precise position measurements in the bending plane. In addition, resistive plate chambers and thin gap chambers with a fast response time are used primarily to trigger muons. The ATLAS trigger system has three levels: the hardware-based Level-1 trigger and the two stage High Level Trigger (Level-2 trigger and Event Filter). Details on the ATLAS detector and trigger system can be found in [3].

3. – Event selection

This analysis searches for Higgs boson candidates by selecting two same-flavour, opposite-sign lepton pairs in an event passing single-lepton or di-lepton triggers. Each electron (muon) must satisfy $E_T > 7\,\text{GeV}$ ($p_T > 6\,\text{GeV}$) with pseudo-rapidity $|\eta| < 2.47(|\eta| < 2.7)$. The first three leptons composing the quadruplet must satisfy the p_T requirement of 20, 15 and 10 GeV. The same-flavour and opposite-sign lepton pair closest to the Z boson mass is referred to as the leading di-lepton and its invariant mass, m_{12}, is required to be between 50 and 106 GeV. The remaining same-flavour, opposite-sign lepton pair is the sub-leading di-lepton and its invariant mass, m_{34}, is required to be in the range $m_{min} < m_{34} < 115\,\text{GeV}$, where m_{min} depends on the reconstructed four-lepton invariant mass, m_{4l}, and varies from 12 to 50 GeV. Cuts on track and calorimetric isolation and on impact parameter significance are applied to reduce the background contamination due to $Z +$ jets and $t\bar{t}$.

The irreducible $ZZ^{(*)}$ background is estimated using MC simulation normalised to the theoretical cross section, while the rate and composition of the reducible $Z +$ jets and $t\bar{t}$ background processes are evaluated with data-driven methods. The composition of the reducible backgrounds depends on the flavour of the sub-leading di-lepton and different approaches are taken for the $ll + \mu\mu$ and the $ll + ee$ final states.

The shape and normalisation of the backgrounds are in good agreement with data [2].

For the measurements of the mass, signal strength, spin and parity no categorization of events has been considered. While to separately measure the cross sections and the couplings for the ggF, VBF, and VH production mechanisms, each Higgs candidate selected with the criteria described above is assigned to one of three categories (VBF-like, VH-like, or ggF-like), depending on its characteristics. The VBF-like category is defined by events with two high p_T jets widely separated in rapidity. Events which do not satisfy the VBF-like criteria are considered for the VH-like category if there is a lepton (e or μ), in addition to the four leptons forming the Higgs boson candidate, with $p_T > 8\,\text{GeV}$ and satisfying the same lepton requirements. Events which are not classified as VBF-like or VH-like are assigned to the ggF-like category.

4. – Properties measurement

An excess of events over the background at $m_H = 124.3\,\text{GeV}$ with a significance of 6.6 standard deviations, corresponding to a background fluctuation probability of 2.7×10^{-11} is clearly visible using only the data related to this decay channel [2].

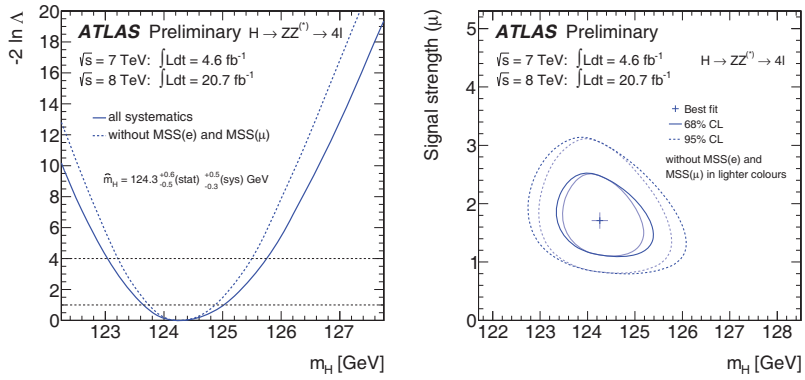

(a) (b)

Fig. 1. – a) The profile likelihood as a function of m_H for the combined $\sqrt{s} = 8\,\text{TeV}$ and $\sqrt{s} = 7\,\text{TeV}$ data samples [2]. The profile likelihoods are shown with (solid curve) and without (dashed curve) the mass scale systematics applied. b) Likelihood ratio contours in the (μ, m_H) plane corresponding to 68% and 95% level contours, shown with (dark colour curves) and without mass scale uncertainties applied (lighter colour curves) [2].

The mass distributions are described using smooth, non-parametric, unbinned estimates [4] of the relevant probability density functions obtained from simulation. The signal shape, normalisation and corresponding uncertainties are parametrised as a function of m_H. The statistical test used is the profile likelihood ratio and is valued using a Maximum Likelihood fit. In fig. 1a) the profile likelihood is shown as a function of m_H for the whole data sample. It is shown with the mass scale systematic uncertainties from electrons (MSS(e)) and muons (MSS(μ)) applied (solid curve) and without applying them (dashed curve). The value for the fitted mass from the profile likelihood is $m_H = 124.3^{+0.6}_{-0.5}(\text{stat})^{+0.5}_{-0.3}(\text{syst})\,\text{GeV}$, where the systematic uncertainty is dominated by the energy and momentum scale uncertainties.

The measurement of the global signal strength factor μ, the ratio of the observed cross section to the expected SM cross section, is presented. Figure 1b) shows the best μ and m_H fit values and the profile likelihood ratio contours that, in the asymptotic limit, would correspond to 68% and 95% confidence levels both with mass scale systematics applied (dark colour curves) and without applying them (lighter colour curves). The value of the signal strength μ at the best fit value for m_H (124.3 GeV) is $\mu = 1.7^{+0.5}_{-0.4}$. For a value of $m_H = 125.5\,\text{GeV}$ [5], the signal strength is found to be $\mu = 1.5 \pm 0.4$.

The measurement of a global signal strength factor can be extended to measure the signal strength factors for specific production modes. The production mechanisms are grouped into the "fermionic" (ggF and $t\bar{t}H$) and the "bosonic" (VBF and VH) modes. In fig. 2a) the best fit values $\mu_{\text{ggF}+t\bar{t}H} \times B/B_{\text{SM}}$ and $\mu_{\text{VBF+VH}} \times B/B_{\text{SM}}$ are presented. The factor B/B_{SM}, the scale factor of the branching ratio with respect to the SM value, is included since with a single channel analysis, the source of potential deviations from the SM expectation cannot be resolved between production and decay. The profile likelihood ratio contours that, asymptotically, correspond to the 68% and 95% confidence levels are also shown. The measured values for $\mu_{\text{ggF}+t\bar{t}H} \times B/B_{\text{SM}}$ and $\mu_{\text{VBF+VH}} \times B/B_{\text{SM}}$ are $1.8^{+0.8}_{-0.5}$ and $1.2^{+3.8}_{-1.4}$, respectively. The ambiguity between production and decay is

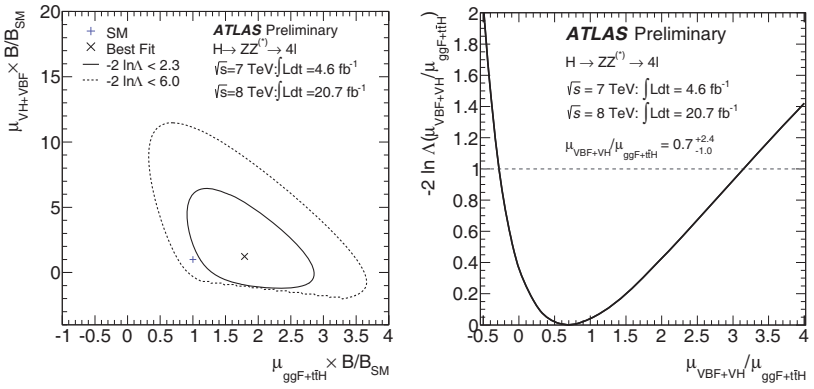

(a) (b)

Fig. 2. – a) Likelihood contours in the $(\mu_{\mathrm{ggF}+t\bar{t}H}, \mu_{\mathrm{VBF+VH}})$ plane including the branching ratio factor B/B_{SM} [2]. b) Results of a likelihood scan for $\mu_{\mathrm{VBF+VH}}/\mu_{\mathrm{ggF}+t\bar{t}H}$ [2].

removed in fig. 2b), where the ratio $\mu_{\mathrm{VBF+VH}}/\mu_{\mathrm{ggF}+t\bar{t}H}$ is presented. The measured value of this ratio is $0.7^{+2.4}_{-1.0}$.

For $H \to ZZ^{(*)} \to \ell^+\ell^-\ell^+\ell^-$ decays, the observables sensitive to the underlying spin and parity of Higgs-like observed particle are the masses of the two Z bosons, the production angle (θ^*) and four decay angles (Φ_1, Φ, θ_1 and θ_2). The production and decay angles are shown in fig. 3a) and they are defined as: θ_1 (θ_2) is the angle between the negative final state lepton and the direction of flight of Z_1 (Z_2) in the Z rest frame; Φ is the angle between the decay planes of the four final state leptons expressed in the four lepton rest frame; Φ_1 is the angle defined between the decay plane of the leading lepton pair and a plane defined by the vector of the Z_1 in the four lepton rest frame and the

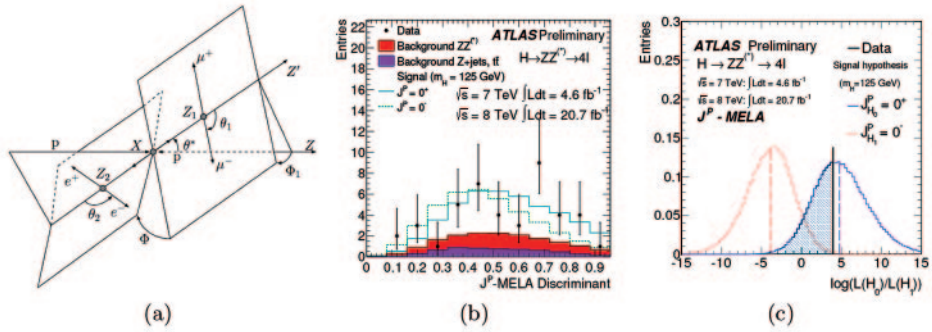

(a) (b) (c)

Fig. 3. – a) Definition of the production and decay angles in an $X \to ZZ^{(*)} \to 4l$. The illustration is drawn with the beam axis in the lab frame, the Z_1 and Z_2 in the X rest frame and the leptons in their corresponding parent rest frame [6]. b) Examples of distributions of the J^P-MELA discriminants showing the 0^+ *versus* 0^- hypothesis for data and Monte Carlo expectations [2]. c) Distributions of the log-likelihood ratio generated with more than 500k Monte Carlo pseudoexperiments when assuming the spin-0^+ hypothesis and testing the 0^- for J^P-MELA (plot b) [2].

positive direction of the parton axis; θ^* is the production angle of the Z_1 defined in the four lepton rest frame [6]. The current collected data do not allow a direct measurement of the coupling parameters. Hence a first step is understanding the spin-parity of the resonance, distinguishing between two different hypotheses using multivariate techniques. Six hypotheses for spin-parity have been tested, namely $0^{\pm}$, $1^{\pm}$, $2^{\pm}$ with candidate events in the region $115\,\text{GeV} < m_{4l} < 130\,\text{GeV}$. The test statistic used is the log-likelihood ratio $\ln[L(H_1)/L(H_0)]$, where H_0 is the SM hypothesis and H_1 the alternative one. Two approaches have been pursued to develop the discriminants used to distinguish between the pairs of spin-parity states: one uses the theoretical differential decay rate for the angles, m_{12} and m_{34}, corrected for detector acceptance and analysis selection, to construct a matrix element based likelihood ratio (MELA) [6] as a discriminant between the different spin-parity hypotheses; the other uses a boosted decision tree (BDT) in a multivariate analysis [2]. The discrimination between the different hypotheses has been studied using MC pseudo-experiments and the production mode is assumed to be 100% ggF.

Figure 3 shows an example of the J^P-MELA discriminant distributions for 0^+ and 0^- hypotheses (plot a) and of the log-likelihood ratio distribution (plot b) generated with more than 500k Monte Carlo pseudoexperiments when assuming the spin-0^+ hypothesis and testing the 0^-. In each experiment the expected numbers of signal and background events are fixed to the observed yields. The log-likelihood value observed in the data is indicated by the solid vertical line, and the medians of each of the expected distributions are indicated by dashed lines. The shaded areas correspond to the observed p_0-values, representing the compatibility with the tested hypothesis H_1 and the assumed hypothesis H_0 (left shaded area). The Standard Model 0^+ hypothesis is preferred when compared pair-wise with 0^-, 1^+, 1^-, 2^+, and 2^-. The 0^+ hypothesis has also been compared to the 2^+_m hypothesis for varying fractions of ggF and $q\bar{q}$ production and the expected separation is found to be independent of the production fractions. Both the BDT and J^P-MELA approaches show similar exclusions [2].

REFERENCES

[1] Englert F. and Brout R., *Phys. Rev. Lett.*, **13** (1964) 321; Higgs P. W., *Phys. Rev. Lett.*, **13** (1964) 508; Guralnik G. S., Hagen C. R. and Kibble T. W. B., *Phys. Rev. Lett.*, **13** (1964) 585.

[2] ATLAS Collaboration, ATLAS-CONF-2013-013 (`https://cds.cern.ch/record/1523699`).

[3] ATLAS Collaboration, *JINST*, **3** (2008) S08003; ATLAS Collaboration, *Eur. Phys. J. C*, **72** (2012) 1849, arXiv:1110.1530 [hep-ex].

[4] Cranmer, Kyle S., *Comput. Phys. Commun.*, **136** (2001) 198.

[5] ATLAS Collaboration, ATLAS-CONF-2013-014 (`https://cds.cern.ch/record/1523727`).

[6] Gao Y. *et al.*, *Phys. Rev. D*, **81** (2010) 075022, arXiv:1001.3396 [hep-ph]; Bolognesi S. *et al.*, *Phys. Rev. D*, **86** (2012) 21.